Carbohydrate Research, 239 (1993) 249–256
Elsevier Science Publishers B.V., Amsterdam

Note

Visualisation of the geometries of objects fabricated from calcium alginate, using magnetic resonance imaging

Kimberlee Potter, Nicholas J. Herrod, T. Adrian Carpenter and Laurance D. Hall

Herchel Smith Laboratory for Medicinal Chemistry, Cambridge University School of Clinical Medicine, University Forvie Site, Robinson Way, Cambridge CB2 2PZ (United Kingdom)

(Received December 10th, 1991; accepted June 22nd, 1992)

Magnetic resonance imaging (MRI) is a widely used medical imaging modality[1] that is now starting to be recognised as a valuable tool for non-medical applications. Its potential for mapping the spatial distribution of hydrogen-containing fluids in objects was first demonstrated by Lauterbur[2]. One-, two-, and three-dimensional imaging have since been used to map the spatial distribution of water in such heterogeneous systems as rocks[3–6], polymers[7], and foods[8]. With the development of fast imaging techniques[9–12], it is now possible to produce three-dimensional MRI images within a few minutes.

Image intensity depends on a number of sample-dependent variables, such as the concentration of hydrogen-containing molecules (M_0), the longitudinal (T_1) and transverse (T_2) relaxation times of their protons, and also their relative mobility. In a dilute polysaccharide gel, the distribution of water will generally be approximately constant and hence there will be little or no contrast from a proton density (M_0) map. However, small variations in polysaccharide concentration are known to induce substantial changes in the T_2 response of the water protons[13] within the gel matrix. Therefore, variations in the intensity of a T_2-weighted image provide a qualitative measure of the variation in polysaccharide concentration within the gel[14]. We now show that MRI can be used to visualise the internal structure of various shapes fabricated from calcium alginate and that this structure depends on the external geometry of the object. Since the pore size of calcium alginate depends on the concentration[15], the mapping of alginate concentration has important implications in such fields as biotechnology[16], medicine[17], and agriculture[18] where the mass transport of small molecules into and out of the gel matrix is of interest.

Correspondence to: Professor L.D. Hall, Herchel Smith Laboratory for Medicinal Chemistry, Cambridge University School of Clinical Medicine, University Forvie Site, Robinson Way, Cambridge CB2 2PZ, United Kingdom.

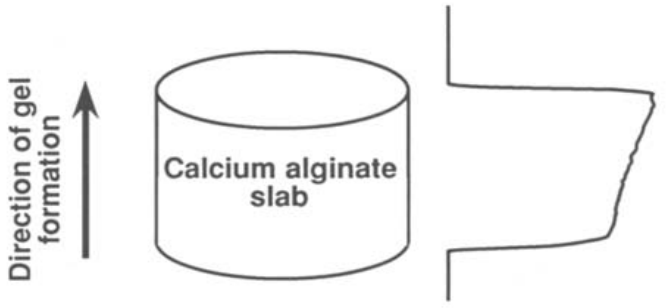

Fig. 1. A one-dimensional profile (at right) of a slab of calcium alginate, in air, taken in the direction of gel formation: TE, 24 ms; field of view (FOV), 5 cm; spatial resolution, 200 μm; acquisition time, 1 s.

The one-dimensional projection image of a slab of calcium alginate in air (Fig. 1), obtained in less than one second, makes it possible to interrogate the variation in the proton signal in just one dimension with high spatial resolution (200 μm). The intensity profile shows a progressive increase in proton signal with distance from the bottom of the slab, which is where the sodium alginate first comes in contact with the calcium chloride solution. It is difficult to decide whether this increase is due to an increase in the cross-sectional area of the gel from the bottom to the top of the slab, or to a variation in the T_2 of the water protons across the gel. Thus, the main disadvantage of this technique is that, since it collapses all the spatial information from the orthogonal imaging plane onto the imaging axis, the shape of the object may influence the observed intensity profile. Nevertheless, this technique is ideally suited for studies of systems for which it is necessary to sacrifice spatial information in order to obtain the data as quickly as possible, e.g., for a system which is changing with time. However, it is preferable for the system to have a uniform cross-section in the orthogonal plane.

In order to investigate further the variation in signal intensity across the calcium alginate slab, a two-dimensional (256 × 256 pixel) slice image [Fig. 2(a)] was taken vertically through the same slab immersed in a beaker of water, using the same

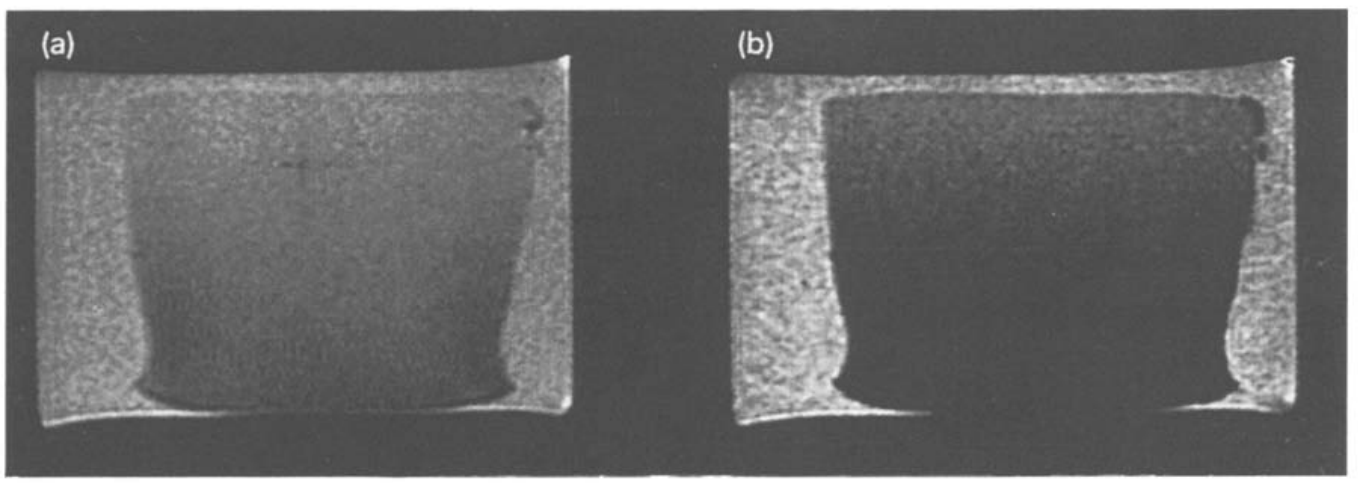

Fig. 2. (a) A two-dimensional slice image of the slab of calcium alginate used in Fig. 1, in a beaker of water (TE, 24 ms; TR, 10 s), and (b) a heavily T_2-weighted image of the same slab (TE, 100 ms; TR, 10 s); slice thickness, 2 mm; FOV, 5 cm; in-plane resolution, 200 μm; acquisition time, 43 min.

echo time (TE 24 ms) as in the one-dimensional experiment. The total imaging time was 43 min. Again, the proton signal increased from the bottom of the slab to the top.

Comparing Fig. 2(a) with Fig. 2(b), taken at a longer TE (100 ms), it can be seen that the decay in image intensity is not uniform across the slab, suggesting that the variation in image intensity is due to a variation in T_2 of the water protons in the gel. This was confirmed by acquiring a series of profiles, including the one shown in Fig. 1, for various echo times (TE 18, 24, 36, 56, 76, and 100 ms), and fitting the results to a single exponential decay curve of the form:

$$M = M_0 \exp(-TE/T_2) + \text{constant}.$$

The proton density (M_0) and the T_2 values of the water protons within the gel are given in Figs. 3(a) and 3(b), respectively.

Since T_2 of the water protons in the gel is related to gel concentration[13], the above results imply that the alginate concentration varies significantly in the direction of gel formation. This observation is consistent with a previous report[19] where physical sectioning of specimens followed by gravimetric analysis was used to demonstrate variations in alginate concentration for gel cylinders.

A T_2-weighted image taken horizontally through a monolayer of calcium alginate beads (diameter 3–4 mm) immersed in a beaker of water (Fig. 4) also showed a marked difference in image intensity between the edges of the beads and their centres. This variation in intensity reflects a dramatic change in T_2 (and hence alginate concentration). These results are again consistent with the literature[16] which states that, because of their small size, the alginate concentration gradients inside such beads are much steeper than that inside a thick slab. Although no experimental evidence was presented to support this claim, those concentration gradients can now be readily visualised in Fig. 4.

In order to study objects which have an irregular or convoluted structure, it is often necessary to acquire a three-dimensional (3D) volume data set, which can be achieved in a few minutes using a fast imaging technique; it can then be viewed from any direction, or "sliced" at any angle using computer software. Furthermore, external features can be defined by shaded-surface volume-rendering. All of these features are illustrated in Fig. 5, for a thread (diameter 5–6 mm) of calcium alginate (dark) suspended in a cylinder of water (bright). The resulting images are heavily T_2-weighted, which gives good image contrast between the surrounding water and the thread. The image in Fig. 5(a) shows a perspective view of the 3D data set in which both the thread and the surrounding water can be seen. Figs. 5(b) and 5(c) show two typical slice images abstracted from the 3D data set which clearly delineate the location of the alginate thread, inspection of which indicates, as before, that the gel is heterogeneous across the diameter of the thread. In Fig. 5(d), the thread has been segmented from the original data set so it can be visualised separately from the water; however, only the external surface of the thread can be seen.

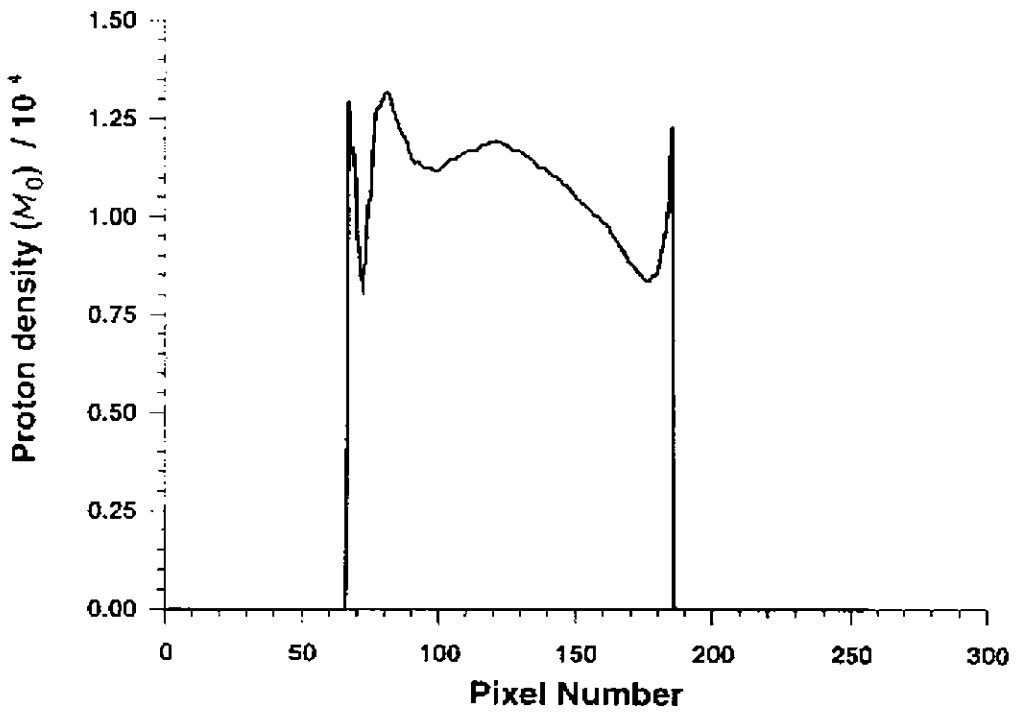

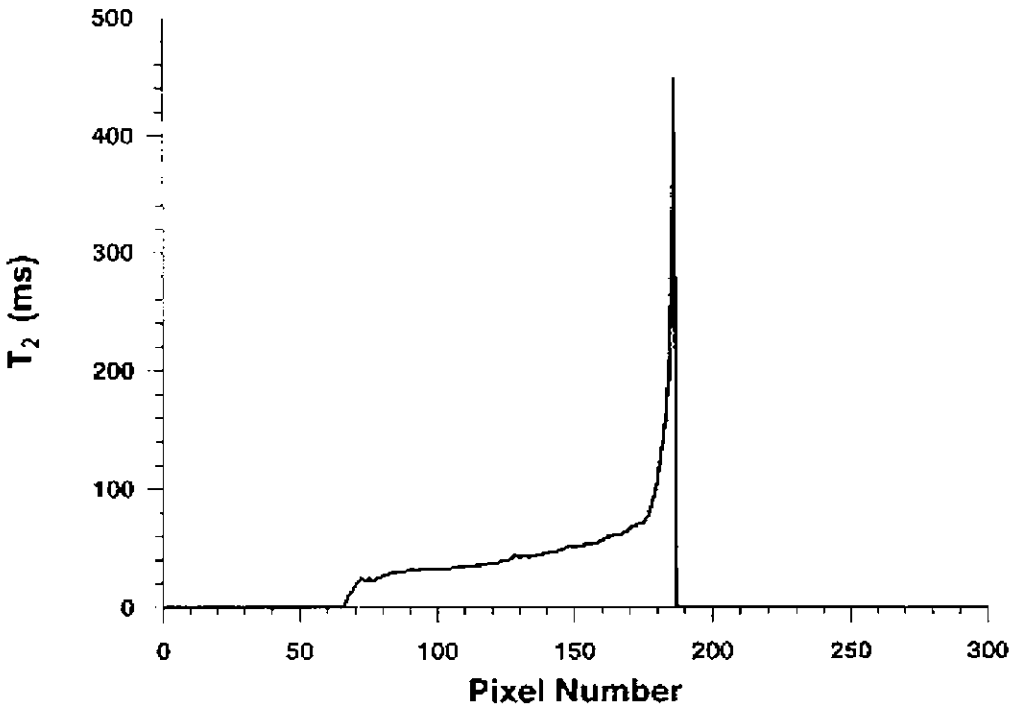

Fig. 3. (top) A one-dimensional proton density (M_0) map for the alginate slab used in Fig. 1 and (bottom) a one-dimensional map of the T_2 values of the water protons in the gel. The direction of gel formation is from left to right and the pixel resolution was 200 μm.

It is evident from the images presented here that the spatial heterogeneity of alginate concentration within the gel matrix can be visualised by the variation of image intensity across the gel. The present findings on alginate gels, coupled with previous reports[13,14] on other polysaccharide gels, encourages us to believe that the MRI signal intensity of water can give a direct quantitative measure of the concentration of polysaccharides in gel matrices. It is also clear that the external structure of an object fabricated from calcium alginate affects its internal structure, which corroborates the previous work of Skjåk-Bræk et al.[19].

EXPERIMENTAL

Samples.—Calcium alginate gels were prepared from an aq 3% (w/v) solution of sodium alginate (Fisons), treated with 0.06 M $CaCl_2 \cdot 6H_2O$ (Fisons A.R. Grade). Slabs of calcium alginate were fabricated by pouring the sodium alginate solution into a plastic cylinder (i.d. 32 mm, height 24 mm) with a dialysis membrane at one end, and dialysing against aq $CaCl_2$ (ref. 20). Beads (diameter 3–4 mm) were prepared by adding the sodium alginate solution dropwise to $CaCl_2$ solution[21]. Threads were formed by forcing the sodium alginate solution through the orifice of a 100-mL syringe located near to the surface of a solution of $CaCl_2$. In each preparation, the calcium alginate was allowed to set for at least 24 h. The bulk T_1 of the water protons in a slab of calcium alginate gel, measured by inversion recovery, was 2 s; the bulk T_2, measured using a spin-echo sequence with varying echo times, was 130 ms.

Imaging.—All MRI experiments were conducted using an Oxford Research Systems BIOSPEC I imaging spectrometer coupled to an Oxford Instruments 310-mm horizontal-bore, superconducting magnet operating at 2.0 T (83.7 MHz for

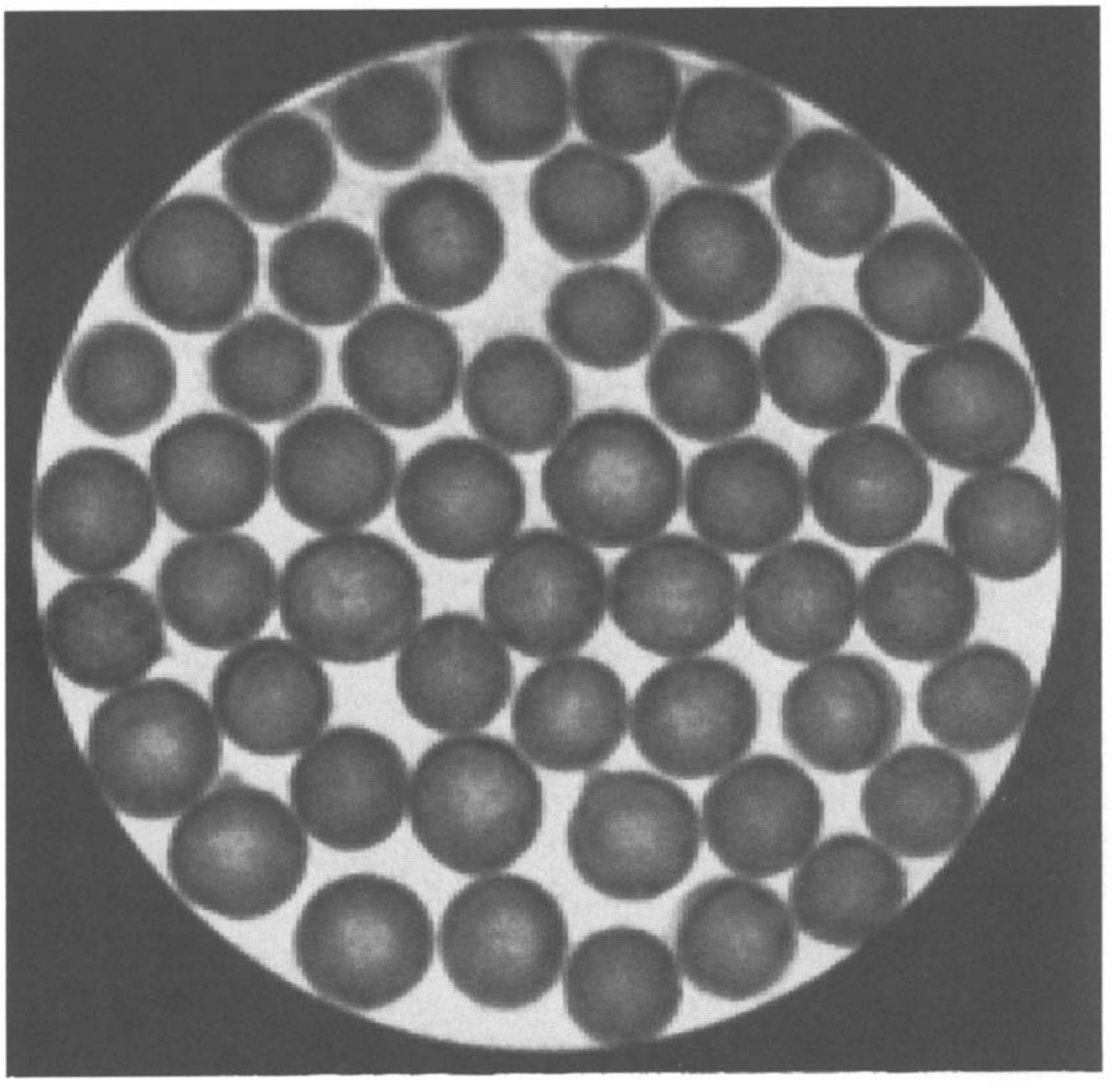

Fig. 4. A two-dimensional T_2-weighted image of a monolayer of calcium alginate beads (diameter 3–4 mm) in a beaker of water: TE, 100 ms; TR, 10 s; slice thickness, 2 mm; FOV, 5 cm; in-plane resolution, 200 μm; acquisition time, 43 min.

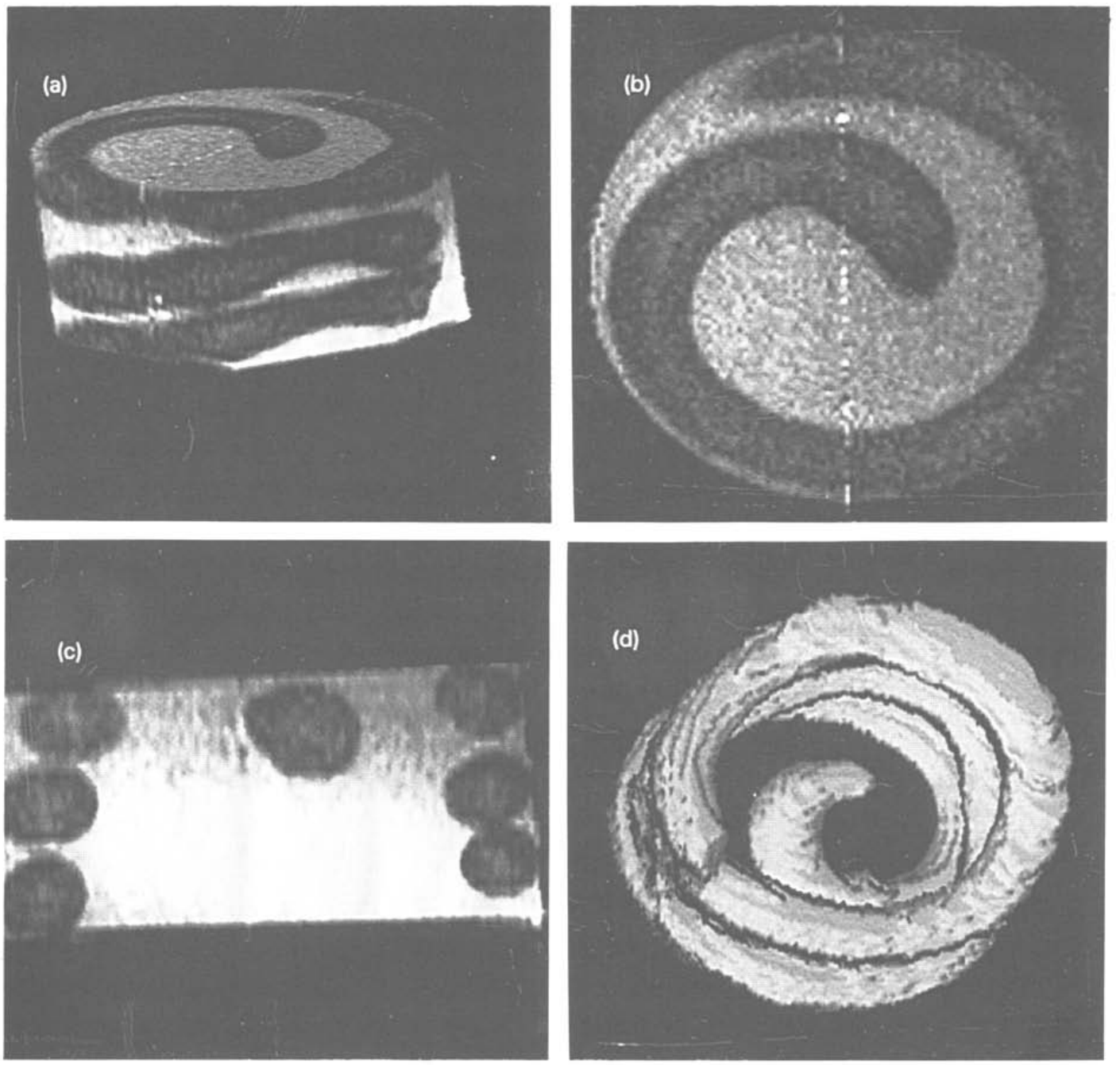

Fig. 5. (a) A three-dimensional volume image of a thread of calcium alginate (dark) suspended in a beaker of water (bright), (b) a slice taken horizontally, (c) a slice taken vertically through the data set, and (d) a shaded surface display of the alginate thread after segmentation from the surrounding water.

^{1}H). Imaging magnetic field gradients in three orthogonal directions were supplied by a custom built Helmholtz–Golay gradient set[22] (i.d. 200 mm), and all samples were studied using a split-ring resonator probe[23] (i.d. 60 mm, height 115 mm) placed with its long axis vertical in the bore of the gradient set.

The one-dimensional projection image[2] (Fig. 1) of an alginate slab in air was obtained using a Hahn spin-echo sequence[24], with an echo time (TE) of 24 ms, in the presence of a uniform magnetic field gradient (1.0 Gauss/cm) oriented perpendicular to the alginate slab. The projection image represents a 5-cm field of view, resulting in a spatial resolution of 200 μm along the cylindrical axis of the slab.

Two-dimensional slice images were acquired using a conventional "spin-warp" imaging sequence[25] utilising a 3-lobe slice-selective 180° sinc pulse. Different

amounts of T_2 contrast were introduced by keeping the recycle delay (TR) constant at 10 s and varying TE from 24 [Fig. 2(a)] to 100 ms [Figs. 2(b) and 4]. These slice images, represented by 256×256 pixel elements, have a slice thickness of 2 mm, and a field of view of 5 cm, corresponding to an in-plane resolution of ~ 200 μm. The acquisition time for each was ~ 43 min.

The three-dimensional ($128 \times 64 \times 128$ voxel) volume data set of an alginate thread suspended in a cylinder of water (Fig. 5) was acquired in ~ 7 min, using a missing pulse steady-state free precession technique[12] (MPSSFP) with a 1-s recycle delay, a TE of 28 ms, and a flip angle of 45°. The in-plane resolution of a horizontal (128×128 pixel) slice abstracted from the 3D data set [Fig. 5(b)] was 400 μm; for a vertical (128×64 pixel) slice, shown in Fig. 5(c), the in-plane resolution was 400×800 μm. The thread shown in Fig. 5(d) was visualised by computer-assisted segmentation of the original data set and subsequent shaded-surface display.

Computing.—All image data were processed on a Sun 4/150 TAAC workstation, using the TAAC accelerator Volume Toolkit in addition to in-house "CaMReS" software. Relaxation data were fitted using in-house software based on the Levenburg–Marquardt nonlinear least-squares minimisation algorithm[26].

ACKNOWLEDGMENTS

It is a pleasure to thank Dr. Herchel Smith for a munificent benefaction (L.D.H. and T.A.C.) and studentship (K.P.). We thank the ORS Award Scheme for additional financial support (K.P.), the Beebe Fund of Cambridge University for a Fellowship (N.J.H.), Mike Tyzska for technical advice, Suzanne Duce for helpful discussions, and John Attard for the curve-fitting software.

REFERENCES

1 P. Mansfield and P.C. Morris, in J.S. Waugh (Ed.), *NMR Imaging in Biomedicine,* in *Advances in Magnetic Resonance, Suppl. 2,* Academic Press, New York, 1982.
2 P.C. Lauterbur, *Nature (London),* 242 (1973) 190–191.
3 R.J. Gummerson, C. Hall, W.D. Hoff, R. Hawkes, G.N. Holland, and W.S. Moore, *Nature (London),* 281 (1979) 56–57.
4 W.P. Rothwell and H.J. Vinegar, *Appl. Optics,* 24 (1985) 3969–3972.
5 L.D. Hall, V. Rajanayagam, and C. Hall, *J. Magn. Reson.,* 68 (1986) 185–188.
6 M.A. Horsfield, C. Hall, and L.D. Hall, *J. Magn. Reson.,* 87 (1990) 319–330.
7 P. Jackson, J.A. Barnes, N.J. Clayden, T.A. Carpenter, L.D. Hall, and P.J. Jezzard, *J. Mat. Sci., Lett.,* 9 (1990) 1165–1168.
8 S.L. Duce, T.A. Carpenter, L.D. Hall, R.C. Hawkes, N.J. Herrod, and M. Tyszka, *Chem. Ind. (London),* 4 (1990) 94–95.
9 P. Mansfield and I.L. Pykett, *J. Magn. Reson.,* 29 (1978) 355–373.
10 A. Haase, J. Frahm, D. Matthaei, W. Hänicke, and K.-D. Merboldt, *J. Magn. Reson.,* 67 (1986) 258–266.
11 R.C. Hawkes and S. Patz, *Magn. Reson. Med.,* 4 (1987) 9–23.
12 S. Patz, S.T.S. Wong, and M.S. Roos, *Magn. Reson. Med.,* 10 (1989) 194–209.

13 W. Derbyshire and I.D. Duff, *Discuss. Faraday Soc.*, 57 (1974) 243–254.
14 S.L. Duce, T.A. Carpenter, and L.D. Hall, *Carbohydr. Res.*, 205 (1990) c1–c4.
15 H. Tanaka, M. Matsumura, and I.A. Veliky, *Biotechnol. Bioeng.*, 26 (1984) 53–58.
16 O. Smidsrød and G. Skjåk-Bræk, *Trends Biotechnol.*, 8 (1990) 71–78.
17 M.F.A. Goosen, G.M. O'Shea, H.M. Gharpetian, S. Chou, and A.M. Sun, *Biotechnol. Bioeng.*, 27 (1984) 147–150.
18 J.A.A. Fujii, D.T. Slade, K. Redenbaugh, and K.A. Walker, *Trends Biotechnol.*, 5 (1987) 335–339.
19 G. Skjåk-Bræk, H. Grasdalen, and O. Smidsrød, *Carbohydr. Polym.*, 10 (1989) 31–54.
20 A. Martinsen, G. Skjåk-Bræk, and O. Smidsrød, *Biotechnol. Bioeng.*, 33 (1989) 79–89.
21 G. Skjåk-Bræk, O. Smidsrød, and B. Larsen, *Int. J. Biol. Macromol.*, 8 (1986) 330–336.
22 T.A. Carpenter, L.D. Hall, and P. Jezzard, *J. Magn. Reson.*, 84 (1989) 383–387.
23 L.D. Hall, T. Marcus, C. Neale, B. Powell, J. Sallos, and S.L. Talgala, *J. Magn. Reson.*, 62 (1985) 525–528.
24 E.L. Hahn, *Phys. Rev.*, 80 (1950) 580–594.
25 W.A. Edelstein, J.M.S. Hutchinson, G. Johnson, and T. Redpath, *Phys. Med. Biol.*, 25 (1980) 751–756.
26 W.H. Press, S.A. Flannery, S.A. Teukolsky, and W.T. Vetterling, *Numerical Recipes in C: The Art of Scientific Computing*, Cambridge University Press, New York, 1988, Chap. 8.